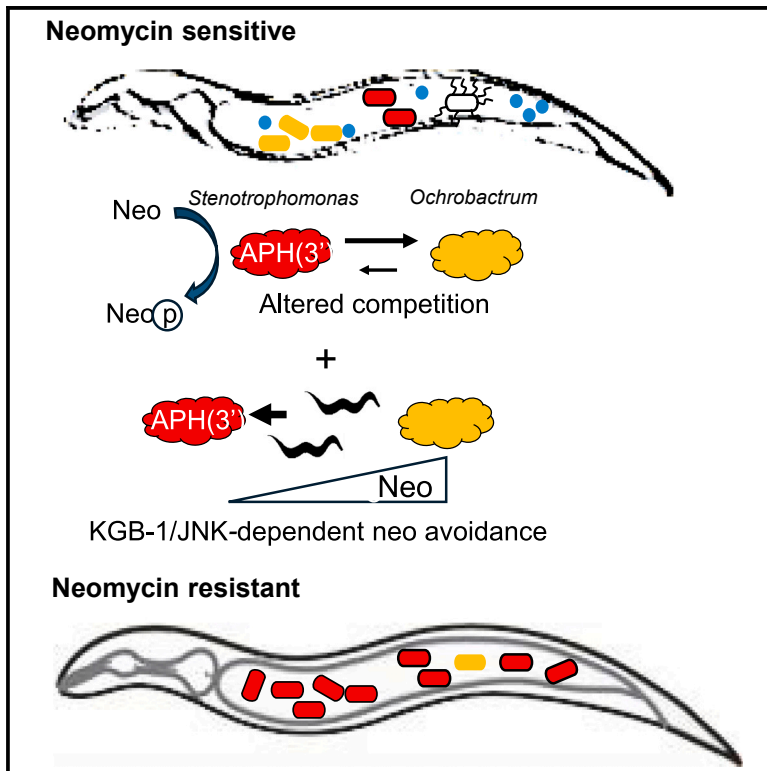


# Gut microbiome remodeling provides protection from an environmental toxin

## Graphical abstract



## Authors

Dan Kim, Sarah El Khoury, Olga Maria Pérez-Carrascal, ..., Lila Wijaya, Kenneth Trang, Michael Shapira

## Correspondence

mshapira@berkeley.edu

## In brief

Microbiology; Microbiome

## Highlights

- Enrichment of toxin-neutralizing gut bacteria protects the host from neomycin toxicity
- Enrichment is driven by altered competitive balance in the gut
- Enrichment is promoted also by KGB-1/JNK-dependent changes in host behavior
- Toxin-protective microbiome remodeling can have detrimental consequences



## Article

# Gut microbiome remodeling provides protection from an environmental toxin

Dan Kim,<sup>1</sup> Sarah El Khoury,<sup>1</sup> Olga Maria Pérez-Carrascal,<sup>1,2</sup> Catherin DeSousa,<sup>1</sup> Da Kyung Jung,<sup>1</sup> Seneca Bohley,<sup>1</sup> Lila Wijaya,<sup>1</sup> Kenneth Trang,<sup>1</sup> and Michael Shapira<sup>1,3,\*</sup>

<sup>1</sup>Department of Integrative Biology, University of California, Berkeley, Berkeley, CA 94720, USA

<sup>2</sup>Present address: Aquatic Geomicrobiology, Institute of Biodiversity, Friedrich Schiller University, Jena, 07743, Germany

<sup>3</sup>Lead contact

\*Correspondence: [mshapira@berkeley.edu](mailto:mshapira@berkeley.edu)

<https://doi.org/10.1016/j.isci.2025.112209>

## SUMMARY

Gut microbiomes contribute to animal health and fitness. The immense biochemical diversity of bacteria holds particular potential for neutralizing environmental toxins and thus helping hosts deal with new toxic challenges. To explore this potential, we used *Caenorhabditis elegans* harboring a defined microbiome, and the antibiotic neomycin as a model toxin, differentially affecting microbiome strains, and also toxic to worms. Worms exposed to neomycin showed delayed development and reduced survival but were protected when colonized with neomycin-resistant *Stenotrophomonas*. 16S rRNA sequencing, bacterial load quantification, genetic manipulation, and behavioral assays showed that protection was linked to enrichment of *Stenotrophomonas* carrying a neomycin-modifying enzyme. Enrichment was facilitated by altered bacterial competition in the gut, as well as by KGB-1/JNK-dependent behavioral changes. While microbiome remodeling conferred toxin resistance, it was associated with reduced infection resistance and metabolic changes. These findings suggest that microbiome adaptation can help animals cope with stressors but may have long-term consequences that add to effects of direct intoxication.

## INTRODUCTION

Animals harbor large gut microbial communities—microbiomes, which are important for their health and fitness. In vertebrates, the gut microbiome has been shown to contribute to processes as diverse as development, immunity, metabolism, and even mood regulation.<sup>1–4</sup> In herbivores (both vertebrate and invertebrates), gut bacteria are essential for mere survival, as energy harvest from plants depends on bacterial enzymes.<sup>5–7</sup> While current understanding highlights how interwoven are the fates of animals and their gut bacteria, the full scale of this dependence is yet unknown. To consider some numbers, the human gut microbiome is estimated to consist of as many bacteria as there are cells in the body and to encode 100-fold more genes than there are in the human genome.<sup>8</sup> Thus, it is likely that our current understanding of the contributions of the gut microbiome represents only the tip of an iceberg.

Host-adapted symbionts, such as those of sap-eating aphids, open new niches by providing their hosts with essential nutrients otherwise missing in available diet, or provide protection from local threats.<sup>9</sup> Niche adaptation can be facilitated also by looser interactions with gut bacteria. Adaptation to toxins is a case in point. To deal with chemically-diverse toxins, animals possess several families of detoxifying enzymes with relatively broad substrate specificity, for example the cytochrome P450 superfamily.<sup>10</sup> However, the repertoire of such enzymes is limited. Bacteria, on the other hand, as a group offer a far greater biochemical

diversity, which throughout animal evolution has been instrumental in enabling host adaptation to toxins, particularly to plant toxins. Examples include the coffee berry borer, a pest of the coffee industry, which is among the few herbivorous insects that are not deterred by caffeine, attributed to the metabolizing activity of *Pseudomonas fulva* gut commensals; or the beetle *Psylliodes chrysocephala*, a major pest of oilseed rape, which is protected from plant isothiocyanates by *Pantoea* commensals; or the Mojave desert woodrat, which can subsist on the otherwise toxic creosote bush, thanks to yet uncharacterized gut commensals.<sup>11–13</sup>

The last century has exacerbated the challenge of environmental toxins, with an expansion in human-made chemicals, such as pesticides, flame retardants, or even antibiotics (of which many are synthetic or semi-synthetic). Some of the released chemicals have intended toxic effects on pathogens or pests but may also have off-target toxicity, others are thought to be toxic but data are ambiguous, and many others have not yet been characterized for possible toxic effects. Such environmental toxins represent novel paradigms of toxicity and stress for animals (including humans) as they contaminate large areas in a short time and spread through water.<sup>14</sup> The timescale of such exposures further reduces the potential of genetic variation within animal populations to be useful. Bacteria, with their biochemical diversity and short generation time are better suited to offer a solution. Examples of bacteria-mediated protection from environmental toxins are still scarce. In the bean bug



*Riptortus pedestris*, a soybean pest, resistance to organophosphate pesticides was found to appear through rapid acquisition of pesticide-metabolizing *Burkholderia*, attributed to their increased environmental abundance in sprayed fields.<sup>15,16</sup> In another study, experimental evolution investigation of the wasp *Nasonia vitripennis* through generations of exposure to sub-toxic concentrations of the herbicide atrazine revealed increased resistance that was provided by gut enrichment for toxin-degrading *Serratia marcescens* and *Pseudomonas protegens*.<sup>17,18</sup> However, the paths and molecular underpinnings of microbiome-mediated protection are not well understood.

We employed a model host and a model toxin to explore the mechanisms leading to bacteria-mediated protection from a novel toxin. As a host model we used the nematode *Caenorhabditis elegans*, a recently established model for microbiome research, shown to harbor a diverse yet characteristic gut microbiome shaped by environmental availability, host genetics and interbacterial interactions.<sup>19–25</sup> *C. elegans* is also increasingly used for studying evolutionary processes that shape host-microbe and host-microbiome interactions.<sup>26–28</sup> As a convenient model toxin we chose neomycin, an aminoglycoside antibiotic, bound to affect the structure and function of the gut microbiome, with sensitive community members inhibited, and resistant members capable of modifying and neutralizing it. Unlike most antibiotics, neomycin is also toxic to worms, offering the opportunity to examine microbiome-mediated protection.<sup>29</sup> The experiments described further demonstrate that rapid bacteria-mediated protection can emerge through distinct mechanisms, involving either interbacterial competition or changes in host behavior, both leading to reproducible microbiome remodeling and enrichment for protective bacteria, and both largely independent of environmental enrichment for protective bacteria. The straightforwardness of these mechanisms suggests that bacteria-mediated protection may be more common than currently appreciated. At the same time, we considered that changes in microbiome composition may also cause dysbiosis, which is often associated with pathology.<sup>30,31</sup> Exploring the long-term consequences of microbiome remodeling identified metabolic remodeling, the significance of which is yet unknown. In addition, it identified a trade-off between short-term toxin protection and longer-term susceptibility to infection. Considering such findings in the broader perspective of environmental intoxication suggests that indirect microbiome-dependent effects may compound the outcomes of toxin exposure.

## RESULTS

### Gut bacteria protect *C. elegans* from neomycin toxicity

Worms were raised either on non-colonizing *E. coli* or on CeMbio, a community of twelve characterized worm gut commensals selected to represent the *C. elegans* core gut microbiome.<sup>32,33</sup> *E. coli* OP50 is a standard lab strain sensitive to neomycin. However, members of the CeMbio community varied in their sensitivity/resistance to neomycin, including four strains, boxed in Figure 1A, which maintained growth following neomycin exposure, both on plates and at least to some extent in liquid cultures. Worms raised on *E. coli* showed dose-dependent developmental delays in response to neomycin, attributed to its toxicity

in worms (and differing from another aminoglycoside, kanamycin, which is equally toxic to *E. coli* but not to worms) (Figure 1B). In contrast, worms raised on CeMbio, which develop faster than worms raised on *E. coli*,<sup>34</sup> were protected from neomycin toxicity, showing no developmental delays. Protection from neomycin toxicity could be conferred by gut bacteria, as worms raised on CeMbio and shifted to neomycin as reproducing adults survived significantly longer than worms raised on *E. coli* (Figure 1C and Table S1). This protection was dependent on live bacteria, as worms raised on paraformaldehyde-killed bacteria of the CeMbio community survived neomycin exposure no better than those raised on *E. coli* (Figure S1). Together, these results demonstrate that the gut microbiome assembled from CeMbio can help its host resist neomycin toxicity.

### Neomycin-induced microbiome remodeling involves gut enrichment with protective *Stenotrophomonas* independent of the extent of its environmental availability

Worms were raised without neomycin on monocultures of the four neomycin-resistant strains and shifted as gravid adults to plates with neomycin and *E. coli* as food. Even without further intake, resistant bacteria persisted (and proliferated) in the worm gut and conferred protection from neomycin (Figures 2A and 2A inset; Table S1 and Figure 2). In contrast, *Lelliottia*, a moderately Neo-sensitive strain, could not persist or protect, although it normally is an effective colonizer of worms.<sup>33</sup> This linked bacterial neomycin resistance with the ability to persist and protect the host. While each of the four Neo-resistant strains managed to persist in the gut of neomycin-exposed worms when in monocultures, next-generation 16S rRNA sequencing of gut microbiomes showed that in the context of a community assembled from CeMbio only one of the four — *Stenotrophomonas indicatrix* JUb19, became dominant (Figure 2B and Table S2). The pattern emerging in several similar experiments showed that unlike gut microbiomes in worms raised on CeMbio without antibiotics, which were dominated by *Ochrobactrum*, microbiomes of worms exposed to neomycin were dominated by *Stenotrophomonas* (Figures 2B, 2C left and Table S2). The driving force for the *Stenotrophomonas* enrichment seemed to be distinct from its environmental availability, which changed relatively little in CeMbio lawns with or without neomycin (Figure 2B). Additional experiments, in which worms were raised on CeMbio and colonized in the absence of neomycin, then shifted to neomycin with *E. coli* as food, still showed enrichment of *Stenotrophomonas*, indicating that the change in microbiome composition was due to the effect of neomycin on, or in, the worm gut (Figure 2C right and Table S2).

An experiment similar to those described earlier of worms raised on CeMbio with or without neomycin, but using colony forming units (CFU) counts to estimate the actual number of bacterial cells in the worm gut, again demonstrated that *Stenotrophomonas* became dominant in the intestine of worms exposed to neomycin (Figure 2D). Importantly, the number of gut *Stenotrophomonas* cells in neomycin-exposed worms was larger than the combined number of *Ochrobactrum* and *Stenotrophomonas* in the gut of unexposed worms, and even larger than the number of all gut bacteria. Since *Ochrobactrum* is somewhat

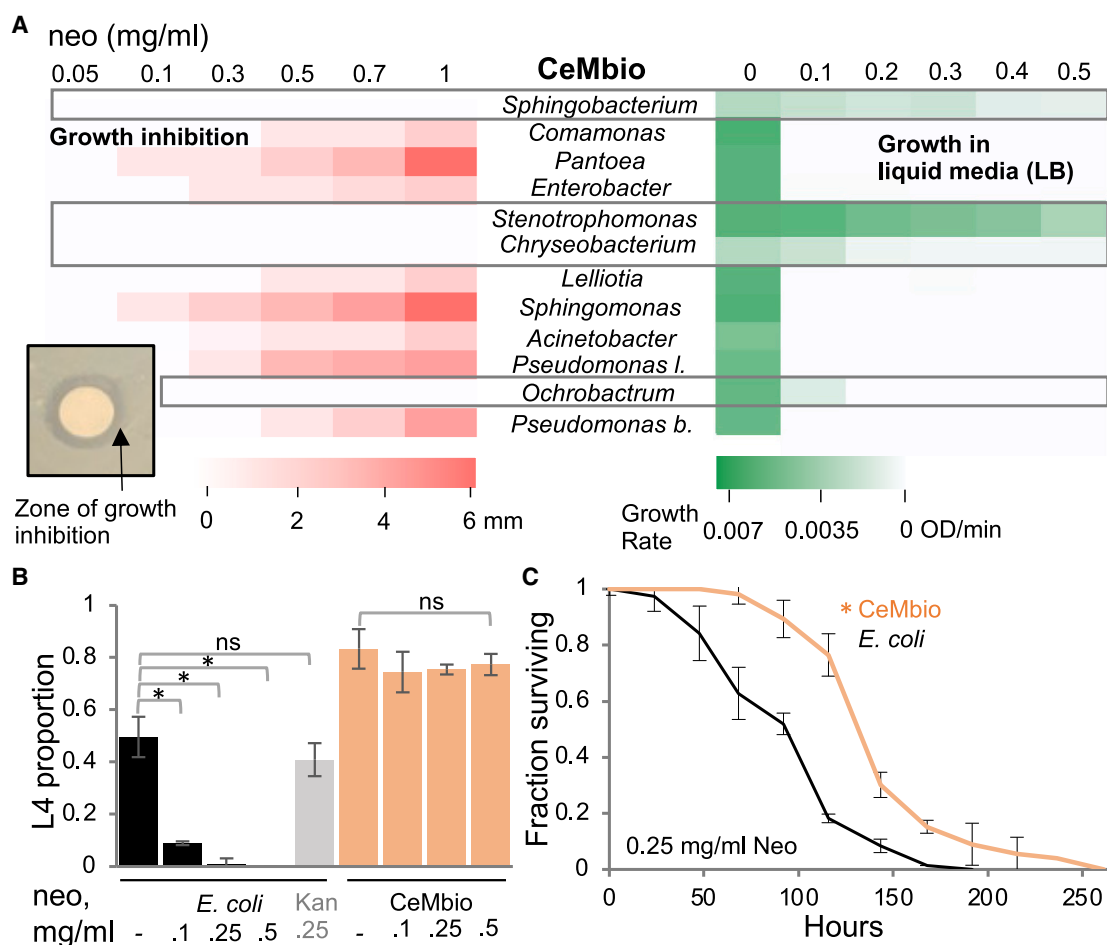


**Figure 1. The gut microbiome protects host from neomycin toxicity**

(A) Sensitivity to neomycin, quantified in CeMbio community members by disk diffusion growth inhibition as demonstrated in inset (red intensity signifies extent of inhibition), or by growth in liquid media (green intensity signifies growth rate). Resistant strains are boxed.

(B) Effects of neomycin (or kanamycin) on development of worms raised on *E. coli* or on CeMbio. Proportion of worms reaching L4 following 30 h of growth from L1 at 20°C. Shown are averages  $\pm$ SD from two independent experiments, each with two plate replicates (total  $n = 4$ ); 17–91 worms/plate; \*,  $p < 7.64 \times 10^{-4}$ , t test.

(C) Survival of wild type worms raised on designated bacterial cultures and shifted as first day gravids ( $t = 0$ ) to plates with neomycin and *E. coli* as food. Shown are averages  $\pm$ SD from three plates (60–73 worms/group); \*,  $p = 1 \times 10^{-10}$ , log-rank test.

resistant to neomycin (Figure 1A) and when in monoculture can persist in the worm gut (Figure 2A inset), its disappearance from the worm gut is not likely due to direct inhibition by neomycin. Instead, this disappearance suggests competitive exclusion by *Stenotrophomonas*, allowing the latter to subsequently allocate more energy for proliferation. *In vitro* competition experiments in liquid culture showed a similar increase in *Stenotrophomonas* growth and displacement of *Ochrobactrum* following addition of neomycin (Figure 3B). Together, these results support the hypothesis that the increase in *Stenotrophomonas* abundance in the gut of neomycin-treated animals was due to its ability to outcompete *Ochrobactrum*.

Scanning the genome of the JUb19 *Stenotrophomonas* strain for potential aminoglycoside-protective mechanisms identified an aminoglycoside 3'-phosphotransferase homolog, APH(3'), which in other bacteria was shown to phosphorylate and neutralize aminoglycosides such as neomycin and kanamycin.<sup>35</sup>

The encoded enzyme may be the factor responsible for JUb19's neomycin resistance and for its ability to protect the host. Worms raised on *Stenotrophomonas* killed with paraformaldehyde were as sensitive to neomycin as those raised on *E. coli*, indicating that active bacterial protein expression was required for protection (Figure 2E). Scanning the genomes of several other *Stenotrophomonas* species (gratefully received from Michael Herman, University of Nebraska), we identified BIGb262, a *Stenotrophomonas rhizophila* strain, also isolated from *C. elegans*, which shared 95.8% of its gene clusters with JUb19, but lacked the APH(3') gene. Unlike JUb19, BIGb262 was sensitive to neomycin and was unable to protect worms from neomycin (Figures 2F and S4A). Transformation of BIGb262 with a plasmid carrying a Kan/Neo<sup>R</sup> selection marker encoded by an APH(3') gene made it resistant to neomycin and capable of protecting worms from neomycin, thus highlighting APH(3') as the likely mechanism through which JUb19 provided protection. Unlike transformed

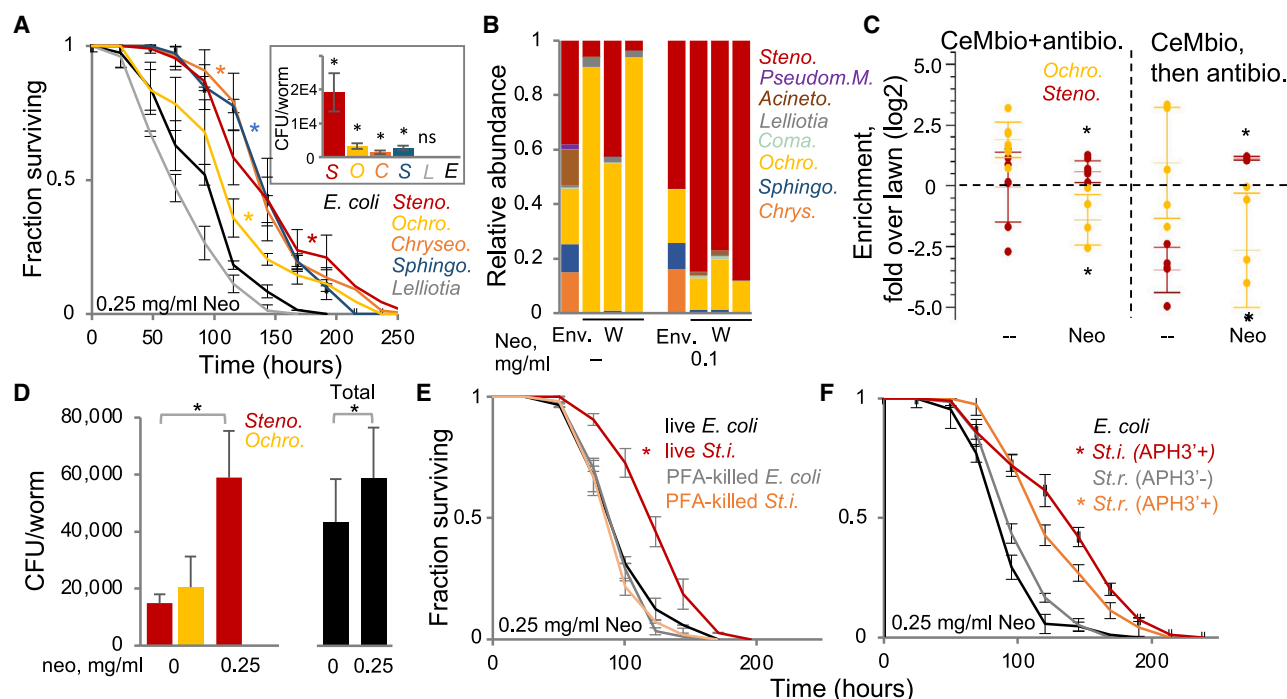


**Figure 2. Neomycin exposure enriches for Neo-resistant gut *Stenotrophomonas***

(A) Survival assays of wild type worms raised on monocultures of Neo-resistant CeMbio strains and shifted as gravids to plates with neomycin and *E. coli* as food. Each curve shows averages  $\pm$ SD from three plates (31–110 worms/group); \*,  $p < 1E-4$ , log-rank test. Inset: Persistence of designated strains in worms 48 h after shift to neomycin plates (10 worms/group, averages  $\pm$ SD for three replicates); \*,  $p < 0.011$ , t test compared to *E. coli*.

(B) A representative experiment showing microbiome composition (analyzed by 16S sequencing, color-coded by strains) in wild type worms raised on CeMbio with or without neomycin (W) or in their lawn environment (Env). Each bar represents a swab of the bacterial lawn or a population of  $\sim 70$  worms.

(C) Gut enrichment of *Ochrobactrum* and *Stenotrophomonas* in worms raised with or without neomycin (left, 3 independent experiments, each with 2–3 separate populations as in B (total  $n = 7$ ), each population marked with a dot), or worms raised on CeMbio and shifted as gravids for 12 h to neomycin with *E. coli* food (right, two independent experiments, 2–3 separate populations each, total  $n = 5$ ). Shown are averages  $\pm$ SD, \*,  $p < 0.05$ , t test.

(D) Bacterial load in gravid worms raised on CeMbio with or without neomycin. CFU counts of gut bacteria cultured on LB with neomycin (left) or without (right); averages  $\pm$ SD for two independent experiments, each with two replicates ( $n = 4$ , 15 worms/experiment); \*,  $p = 0.0018$  (left) and  $p = 0.047$  (right), t test.

(E and F) Survival assays of wild type worms raised on designated bacteria (live or dead) and transferred as gravid to plates with neomycin and *E. coli* food. *St. i.*, *S. indicatrix* (JUB19, APH(3)<sup>+</sup>), *St. r.*, *S. rhizophila* (BIGb262, APH(3)<sup>-</sup>), *St. r.* APH(3)<sup>+</sup>, APH(3)<sup>-</sup>-transformed BIGb262. Each curve shows averages  $\pm$ SD for three plates; 27–45 worms/plate (E),  $N = 44$ –89 worms/plate (F); \*,  $p < 7E-7$ , log-rank test compared to live *E. coli*.

APH(3<sup>-</sup>)-positive BIGb262, a natural colonizer of the worm gut, similarly-transformed non-colonizing *E. coli* OP50 failed to protect worms, in spite of becoming Neo-resistant (Figure 4). Together, these results support the notion that APH(3<sup>-</sup>) expression is what makes *Stenotrophomonas* protective, but that protection depends also on bacterial ability to colonize the worm gut, thus indicating that APH(3<sup>-</sup>) provides protection by neutralizing ingested neomycin.

### Kgb-1-dependent toxin avoidance enables preference and acquisition of neomycin-protective strains

In bacteria, neomycin inhibits protein translation by binding to the 30S ribosomal subunit. To examine how it affected *C. elegans*, we carried out RNA-seq analysis seeking to identify genes that responded to neomycin exposure. Responses were examined 8 h after onset of neomycin exposure to focus on early events, more likely to represent direct effects. DESeq2 analysis identified 82 genes that were downregulated in adult worms exposed to neomycin and 76 that were upregulated (Table S3).

Downregulated genes were primarily enriched for genes annotated with carboxylic acid metabolism process, including genes involved in glycolysis and lipid  $\beta$ -oxidation (corrected  $p$  value of  $5E-10$ ) and for mitochondrial localization ( $p = 0.02$ ), and further included seventeen collagen genes. Upregulated genes were primarily enriched for annotations of defense response to other organism ( $p = E-5$ ) and response to stress ( $p = 2E-4$ ). While it is difficult to determine based on these results how exactly neomycin affected worms, one possible interpretation is that neomycin inhibited some aspects of mitochondrial function, affecting energy metabolism, which activated stress responses. Interestingly, among the upregulated genes, enrichment was found for genes previously characterized as part of the KGB-1 regulon (Table S3).<sup>36</sup> KGB-1 is a stress-activated protein kinase and a JNK homolog that was shown to take part in diverse stress responses in *C. elegans*.<sup>37,38</sup> It was also shown to activate an aversion behavior leading worms away from conditions where essential cellular processes were inhibited.<sup>39</sup> To test whether such avoidance could be activated by neomycin exposure, we



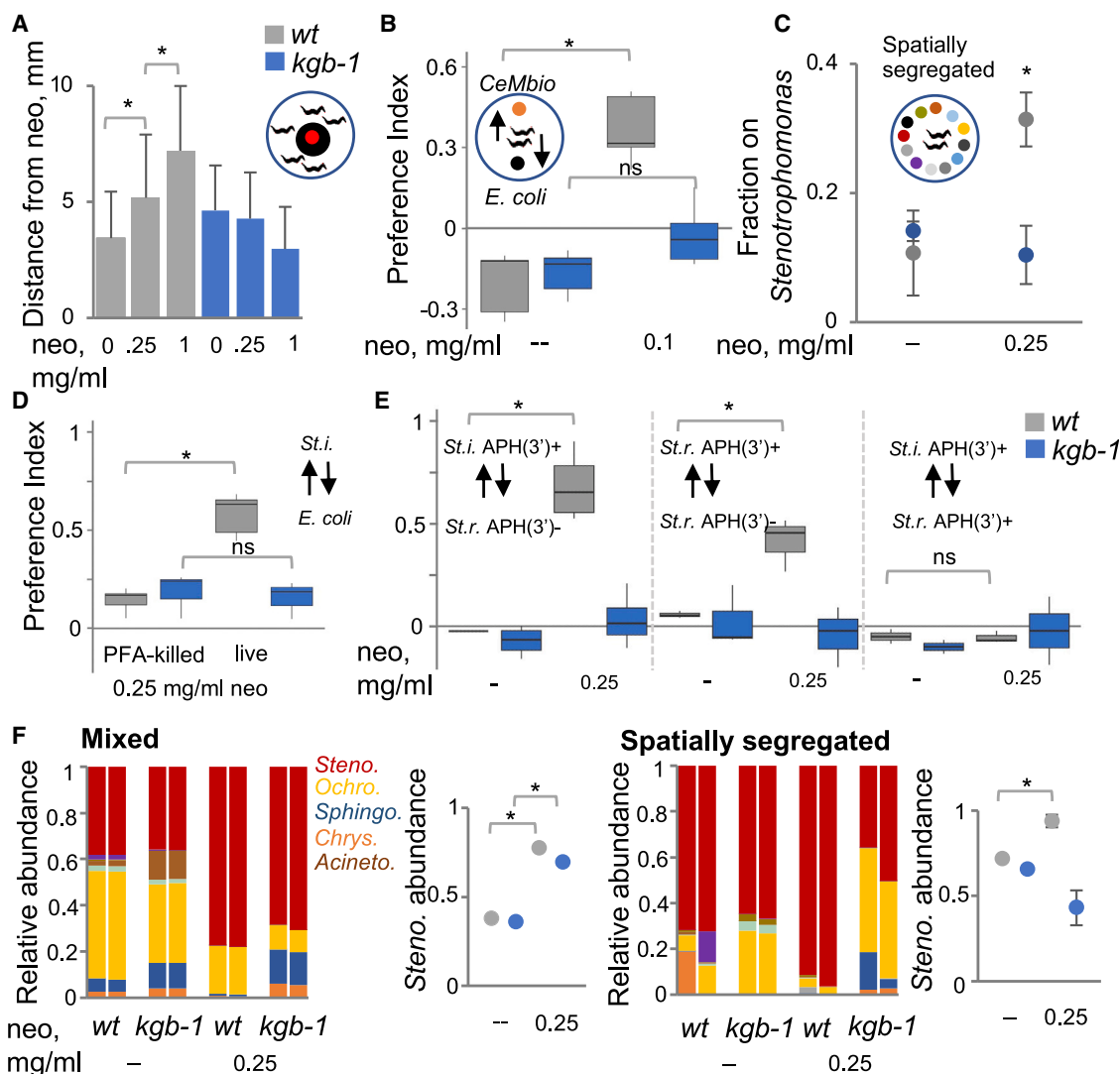


**Figure 3. *kgb-1*-dependent toxin avoidance enables preference and acquisition of Neo-protective *Stenotrophomonas***

(A) Avoidance of neomycin by wild type or *kgb-1* gravid worms within an hour of application. Shown is one experiment, with averages  $\pm$ SD for distances of individual worms from point of neomycin application (red dot on bacterial lawn in scheme); 24–92 worms/group; \*,  $p < 2E-5$ , t test.

(B) Preference assays (direction marked in schemes by arrows) with wild type or *kgb-1* worms between CeMbio and *E. coli*, with or without neomycin. Shown are medians (lines) and interquartile ranges (boxes) for five assay plates from two independent experiments ( $n = 5$ ), 46–134 worms/plate; \*,  $p = 8.5E-5$ , t test.

(C) Preference assay of wild type worms in a multi-choice assay on spatially segregated monocultures of CeMbio members, with or without neomycin. Shown are averages  $\pm$ SD from two independent experiments each with two plate replicates ( $n = 4$ ), 46–185 worms/plate; \*,  $p = 0.01$ , t test.

(D and E) Preference assays with wild type or *kgb-1* worms between *Stenotrophomonas* strains or *E. coli*, live or dead, and with or without neomycin. D. Shown are medians and interquartile ranges for three independent experiments, each with 2–3 assay plates ( $n = 7$ ), 40–157 worms/plate; \*,  $p = 4.5E-7$ , t test. *St. i.*, JU19; *St. r.*, BIGb262; *St. r.* APH(3')<sup>+</sup>, APH(3')<sup>-</sup>-transformed BIGb262. E. Each graph shows medians and interquartile ranges for three assay plates, 37–135 worms/plate; \*,  $p < 0.009$ , t test.

(F) Gut microbiome composition and the derived *Stenotrophomonas* abundance in worms raised on a mixed CeMbio culture, or on spatially segregated monocultures, in plates with or without neomycin. Bar graphs as in Figure 2B, 80 worms/population; *Stenotrophomonas* abundance shows averages  $\pm$ SD of two populations, \*,  $p < 0.05$ , t test.

applied neomycin in different concentrations to worm plates and measured the distance of individual worms from the point of application. This revealed dose-dependent avoidance and further showed that neomycin avoidance was *kgb-1* dependent, supporting activation of KGB-1 by neomycin (Figure 3A). To examine whether this avoidance behavior could play a role in

helping worms acquire protection from neomycin, we carried out preference assays allowing worms to choose between *E. coli* and the neomycin-protective CeMbio community. Unlike adults, larval responses to neomycin were slow, prompting us to extend the time of preference assays, which would allow, in addition to sensing, also involvement of learning processes. By

the end of larval development, in the absence of neomycin, wild-type worms showed a slight preference to *E. coli* over CeMbio. However, neomycin exposure changed that, significantly increasing worm preference for CeMbio, a shift which was *kgb-1* dependent, and further depended on *mek-1*, which encodes KGB-1's upstream activator (Figures 3B, S5 and Table S4). Furthermore, when worms exposed to neomycin were allowed to choose between the twelve members of CeMbio, in this case spatially segregated in random order, a greater percentage of wild-type animals gravitated toward the protective *Stenotrophomonas*, but not so *kgb-1* mutants (Figure 3C). These results supported a role for KGB-1 in responding to the toxic effects of neomycin and activating a behavioral response that led worms away from the toxin, and as a consequence, toward toxin-neutralizing bacteria where concentrations were lower. In agreement with the proposed mechanism, *kgb-1*-dependent preference was only for live *Stenotrophomonas* (Figure 3D) and was tuned to preference of APH(3')-positive *Stenotrophomonas* (Figure 3E). In contrast, the more general preference of live over dead bacteria, observed with non-protective *E. coli*, was independent of *kgb-1* (Figure S6 and Table S4), further supporting a more specific role for KGB-1 in responding to neomycin toxicity.

To test how *kgb-1*-dependent preferences could affect gut microbiome composition, we raised wild type and *kgb-1* worms with or without neomycin, and on *E. coli* or CeMbio—the latter either with all twelve strains mixed, as in Figure 2, or spatially segregated. Whereas both wild type and *kgb-1* mutants showed neomycin-induced *Stenotrophomonas* enrichment when raised on a well-mixed CeMbio, recapitulating the ability of *Stenotrophomonas* to outcompete other strains in the neomycin-affected worm gut, *kgb-1* mutants exposed to neomycin failed to enrich for *Stenotrophomonas* when required to choose between spatially segregated colonies (Figures 3F and Table S4). This distinguishes between two mechanisms which can contribute to enrichment with *Stenotrophomonas*: post-ingestion enrichment seen in mixed cultures, which is independent of *kgb-1*, and a behavioral, *kgb-1*-dependent avoidance that directs worms toward protective bacteria. KGB-1 is expressed both in the gut and in neurons,<sup>40</sup> but the results presented here indicate that its contribution to neomycin-induced changes in microbiome composition were more associated with the latter, although gut-neuron crosstalk is also possible.

### Long-term consequences of neomycin-induced gut microbiome remodeling

Examination of the persistence of neomycin-induced microbiome remodeling demonstrated that worms raised on CeMbio in the presence of neomycin and then shifted away from the toxin maintained a significant *Stenotrophomonas* enrichment for at least two and a half more days, indicating that microbiome remodeling persisted past toxin exposure (Figure 4A). Changes in gut microbiome composition, due to diet, inflammation, or environmental factors, have varied effects on host health and fitness, and are often described as dysbiosis. Therefore, it was of interest to examine how neomycin-induced changes affected host function and fitness. Wild-type worms were raised either on CeMbio, CeMbio with neomycin (to recreate the dysbiotic, *Sten-*

*otrophomonas*-enriched gut microbiome), and on a CeMbio variant reconfigured to emulate the composition of the gut microbiome in worms exposed to neomycin, but without the toxin itself. CFU counts of gut bacteria in worms raised on this reconfigured community demonstrated the desired gut enrichment for *Stenotrophomonas*, although not to the same extent as in neomycin-treated worms (Figure S7). Worms developing on the remodeled microbiomes did not show significant effects on fecundity, or subsequently, on lifespan (Figure S8). However, a significant increase in gut lipid levels was observed in worms raised on *Stenotrophomonas*-enriched communities, representing an increase in energy storage (Figure 4B). A small, non-significant increase was observed in worms raised on CeMbio and exposed to neomycin, but a larger increase was observed in worms raised on the reconfigured CeMbio without neomycin, which was similar to the increase seen in worms raised on *Stenotrophomonas* alone, indicating that *Stenotrophomonas* enrichment was sufficient to alter lipid storage. How this metabolic remodeling may affect host health and fitness is yet unclear. In contrast, the significance of microbiome remodeling for pathogen resistance, as seen with the *Pseudomonas aeruginosa* infection model, was more straightforward. Resistance of *Stenotrophomonas*-enriched worms, in two configurations, was significantly lower than in worms raised on standard CeMbio (Figure 4C and Table S1), and decreased colonization with non-pathogenic bacteria was correlated with the decreased infection resistance (Figure 4C inset). To test whether decreased infection resistance was due to a decrease in community diversity, or alternatively, loss of specific protective strains, we generated three additional modified configurations of the CeMbio community—one that included only strains that were previously shown to prevent pathogenic colonization of *P. aeruginosa*—*Sphingobacterium* strain BIGb0170, *Chryseobacterium* JUb44, and *Pantoea* BIGb0393 (Figure 9),<sup>41</sup> a second community, which lacked only these protective strains, and a third, in which three non-protective strains (*Ochrobactrum* Myb71, *Pseudomonas* MSPm1 and *Sphingomonas* JUb134) were excluded, reducing general diversity, but keeping the three protective strains. The results shown in Figure 4D suggest that loss of infection-protective strains due to neomycin sensitivity is likely the reason for reduced infection resistance following neomycin-driven reconfiguration of the gut microbiome, not a general decrease in microbiome diversity. Thus, while *Stenotrophomonas* enrichment provides short-term toxin protection, displacement of other bacteria represents a trade-off that may have long term negative consequences.

### DISCUSSION

Using neomycin as a convenient model for environmental toxins—toxic to the *C. elegans* host and effectively altering the gut microbiome, our results demonstrate that the gut microbiome can provide protection from an environmental toxin. In the context of a full community, protection was conferred by the most resistant member of the community, a *Stenotrophomonas indicatrix* strain, which outcompeted other gut bacteria and persisted in the affected worm gut. In addition, exposed worms sought relief from the toxin, driven by avoidance behavior that

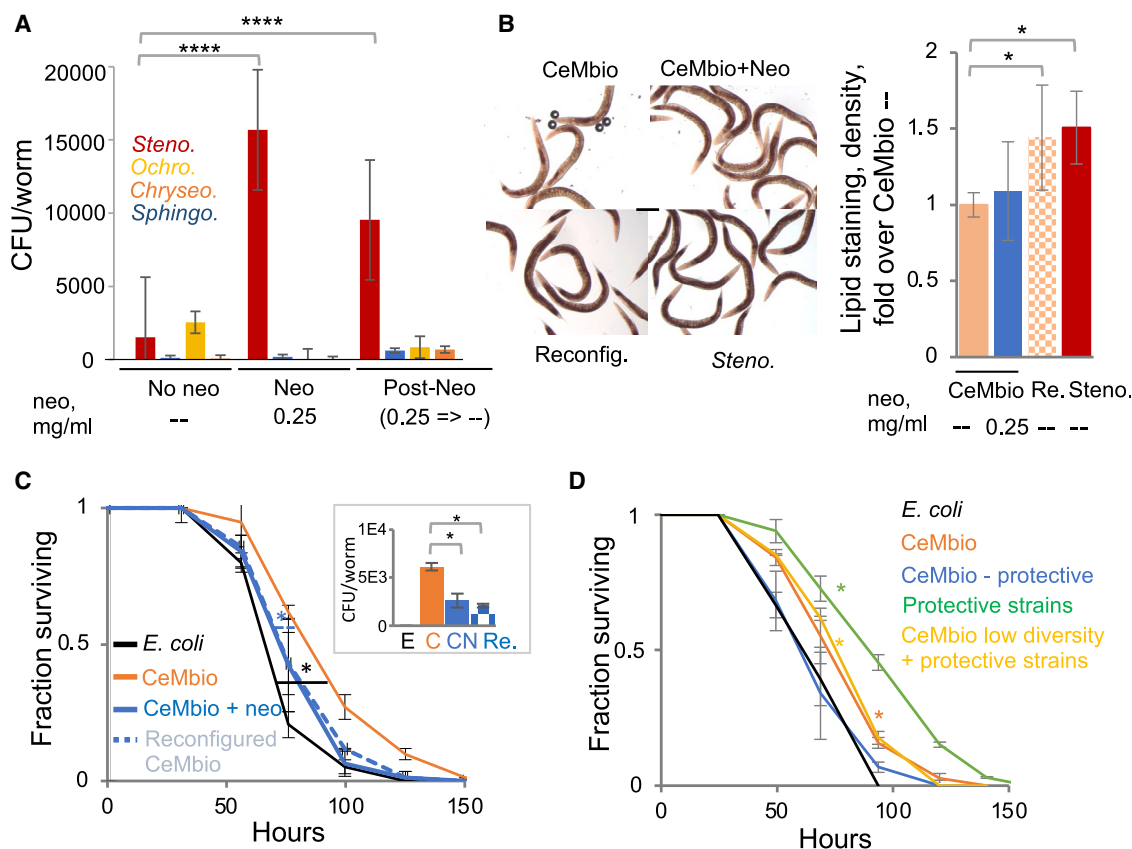


**Figure 4. Consequences of neomycin-induced microbiome remodeling**

(A) CFU counts of gut-colonizing Neo-resistant CeMbio members from worms raised from L1 to mid gravid stage (4.5 days) on CeMbio with or without neomycin, or first with neomycin (two days) and then shifted for 2.5 days more to plates without neomycin (Post-Neo). Averages  $\pm$ SD of two technical repeats per group (13 worms/group); \*\*\*\*,  $p < 0.0001$ , two-way ANOVA followed by a Bonferroni's test.

(B) Left, representative images of lipid staining (proportional to lipid content) in wild type gravid worms raised on CeMbio, on CeMbio with neomycin, on reconfigured CeMbio (Re.) or on *Stenotrophomonas* alone; scale bar, 200  $\mu$ m. Right, quantification of staining in individual worms from three independent experiments. Averages  $\pm$ SD for 16–21 worms/group;  $p = 2.4E-8$ , ANOVA; \*,  $p < 3.7E-05$ , Tukey's HSD post hoc.

(C) Infection resistance in worms raised on designated communities and shifted in adulthood to *Pseudomonas aeruginosa*. Each curve shows averages  $\pm$ SD for three plates (67–83 worms/group);  $p = 1E-7$  (CeMbio vs. *E. coli*),  $p = 0.003$  (CeMbio vs. Re.), log-rank test. Inset. Persistence of CeMbio members in worms 24 h after shift to *P. aeruginosa*. Averages  $\pm$ SD for three technical replicates, 10 worms/group;  $p = 8E-7$ , ANOVA; \*,  $p < 3.4E-05$  Tukey's HSD post hoc.

(D) Infection resistance as in C with worms raised on CeMbio including *Pseudomonas*-protective strains, without them, or without three non-protective strains (low diversity). Curves show averages  $\pm$ SD for three plates (62–87 worms/group), \*,  $p < 3.4E-05$ , log-rank test.

depended on the stress-activated JNK homolog gene *kjb-1*, and that when given a choice resulted in a preference for protective bacteria. Thus, two distinct mechanisms converge to facilitate colonization by protective bacteria. In this toxin-remodeled microbiome, the enrichment for Neo-resistant strains (primarily *Stenotrophomonas*) described a significant deviation from baseline gut microbiome composition, representing dysbiosis. The effects of this dysbiosis on host fitness were limited, with fecundity and lifespan of worms developing on the remodeled community remaining unaltered. However, it did increase the susceptibility of hosts to the pathogen *Pseudomonas aeruginosa*, driven by loss of pathogen-protective but neomycin-sensitive strains, and further altered metabolism leading to increased lipid storage. Our results demonstrate that microbiome-assisted host resistance to environmental toxins is simple and attainable. They further demonstrate that this resistance could arise through

more than one mechanism, either in bacteria or in the host, and that the mechanisms involved are of general purpose—inter-bacterial competition and avoidance of harmful environments, together increasing the likelihood that resistance will emerge. Our results focus on resistance to an environmental toxin, but similar mechanisms could give rise to resistance to other types of environmental stress. At the same time, the results highlight the trade-off that may take place between short-term resistance to the toxin and other adaptive traits, some of which with potential long-term consequences.

The ability of *S. indicatrix* JUB19 to protect worms was associated with its persistence and proliferation in the worm gut, and further associated with its APH(3')-encoding gene. While we did not knock-out the JUB19's APH(3') as a direct demonstration of its requirement for protection, introduction of an APH(3')-encoding gene into *S. rhizophila* BIGb262 showed it to



be sufficient for providing worms with neomycin resistance, as well as to make BIGb262 as attractive to worms as JUb19. While JUb19 was the strain taking over the gut microbiome, the three other Neo-resistant strains were also capable of protecting worms from neomycin. In the case of JUb44 and BIGb170, scanning of gene annotations suggested that they harbored putative neomycin modifying enzymes—an aminoglycoside adenylyltransferase and an unspecified aminoglycoside phosphotransferase, respectively. *Ochrobactrum* Myb71 was also found to harbor a putative APH(3') gene, but unlike JUb44 and BIGb170, Myb71 could not always persist in the worm gut (i.e., under exposure to high neomycin concentrations (0.5 mg/mL)), yet was still able to cf. resistance (Figure 2A, Table S1 and Figure S2). In this case, the ability of Myb71 to protect worms may be associated with its value as food, making the host better able to resist infection on its own, or, as shown in other cases, through activation of host immunity, making the host better prepared for infection.<sup>42</sup> This further demonstrates the potential of bacteria to lend from their biochemical diversity to offer hosts varied solutions to new challenges.

While bacterial environmental availability can be affected by neomycin toxicity, environmental availability was not the main factor responsible for *Stenotrophomonas* gut enrichment, as this occurred also in worms first colonized by CeMbio members and only subsequently exposed to the toxin. The increased bacterial load observed in the toxin-adapted worms is in line with a release from competition and suggests that the mechanism through which *Stenotrophomonas* becomes enriched is its ability to outcompete less-resistant gut bacteria and proliferate on their expense. While previous studies of the bean bug adaptation to pesticide linked host resistance to acquisition of environmentally-enriched protective bacteria,<sup>16</sup> our results demonstrate that when biochemical capabilities pre-exist in the gut microbiome, toxin-induced stress could be sufficient for microbiome remodeling and host protection, independent of environmental availability.

The choice of neomycin as the model toxin and concentrations selected for testing was to ensure microbiome changes in a community with somewhat limited diversity and to ensure observable effects on hosts. In the environment, antibiotic concentrations are usually far lower than those used here.<sup>43,44</sup> Nevertheless, there are examples of antibiotics, specifically aminoglycosides, used in the environment in concentrations as high as those we used.<sup>45</sup> Thus, the mechanisms that we identified as taking part in worm resistance to neomycin might play similar roles in natural contexts. These mechanisms are of general purpose. On the bacterial side, aminoglycoside modifying enzymes are common among bacteria, including in the human gut.<sup>46–49</sup> On the host side, the *C. elegans* stress-activated MAP kinase KGB-1, a JNK homolog, is a conserved protein involved in diverse stress responses as well as in behavioral modulation.<sup>50–52</sup> Together, such mechanisms could facilitate bacteria-dependent resistance to toxic antibiotics in nematodes in the wild, as well as in other animals. Resistance to other toxins may rely on different bacterial toxin-modifying enzymes but could be similarly feasible. And when appropriate enzymes are not as common as those involved in antibiotic resistance, environmental exposure to the toxin could significantly increase

availability of bacteria expressing the appropriate enzyme, as found for the pesticide-resistance bean bug discussed earlier.<sup>16</sup>

While remodeling of the worm gut microbiome provided relief from neomycin toxicity, at least one trade-off was noted, i.e., susceptibility to infection. The case of pathogen susceptibility seems to be straightforward, attributed to loss of bacterial strains that compete better with the pathogen.<sup>41</sup> In addition, the *Stenotrophomonas* enrichment was sufficient to drive metabolic remodeling. The significance of this change is not as clear. Lipid storage is thought to provide energy for worm growth, survival and reproduction, but it has also been shown (following disruption of TORC2 signaling, the less characterized branch of target of rapamycin signaling) to be associated with developmental delays and decreased body size,<sup>53</sup> and in humans, it is associated with metabolic syndrome. Maintaining gut microbiome composition within certain boundaries (still ill-defined) is essential for gut homeostasis,<sup>54</sup> and deviations lead to dysbiosis and pathology.<sup>24,55,56</sup> Host metabolism seems to be sensitive to changes in microbiome composition.<sup>57</sup> The effects of *Stenotrophomonas* enrichment is one example. Work in vertebrates provides many more, linking gut-dysbiosis to metabolic syndrome and obesity.<sup>55,58</sup> Such examples suggest that metabolic remodeling might be a common indirect effect of toxin-induced microbiome-remodeling.

The results presented here support the notion that microbiome-dependent protection from environmental toxins is straightforward, can be achieved through distinct routes and, as a consequence, is probably more prevalent than currently appreciated. Increases in the spread of environmental toxins are only one facet of global change, perhaps representing a change in which bacteria are particularly likely to play a role. However, gut bacteria could contribute to any aspect of physiological and ecological adaptation. The microbiome was previously proposed as a potential source for adaptive novelty.<sup>59</sup> It seems that helping hosts maintain their fitness in a changing environment may be one such contribution. It might be happening all around us, and may further be a yet unaccounted cause of health issues stemming from trade-offs with initially protective remodeling.

### Limitations of the study

The results described provide a proof-of-concept for the straightforwardness of microbiome-dependent toxin resistance, taking advantage of the prevalence of antibiotics resistance mechanisms. When it comes to other toxins, modification mechanisms may be less common and less likely to be available in communities with limited diversity. Nevertheless, in normally diverse environmental microbiomes such mechanisms should be common enough to make microbiome-dependent toxin resistance a phenomenon to be reckoned with and to study.

### RESOURCE AVAILABILITY

#### Lead contact

Further information and requests for resources and reagents should be directed to the lead contact, Michael Shapira ([mshapira@berkeley.edu](mailto:mshapira@berkeley.edu)).

#### Materials availability

All unique/stable reagents generated in this study are available upon request.

# Data and code availability

RNA-seq data generated during this study has been deposited at the Gene Expression Omnibus (GEO) and is publicly available as of the date of publication. The BIGb262 genome sequence was deposited in the NCBI. Accession numbers are listed in the [key resources table](#). This paper does not report original code. Any additional information required to reanalyze the data reported in this paper is available from the [lead contact](#) upon request.

# ACKNOWLEDGMENTS

We thank Dr. Michael Herman and members of his lab in University of Nebraska for providing *Stenotrophomonas* strains, Dr. Dennis Kim—for providing the mutant strain *mek-1(qd375)*, Dr. Britt Koskella—for access to instruments, Dr. Denis Titov—for useful comments and ideas, and Dr. Molly Matty—for technical advice. This work was supported by NIH grants R01OD024780 and R01ES034012. D.K. was supported by National Science Foundation Graduate Research Fellowship Program (DGE 2146752).

# AUTHOR CONTRIBUTIONS

D.K. and M.S. conceived the project; D.K., assisted by S.E.K., S.B., L.W., D.K.J., and K.T., performed all experiments and analyzed the results, except for experiments characterizing infection resistance to *Pseudomonas Aeruginosa*, which were carried out by O.M.P.-C., and lipid staining experiments, which were performed and analyzed by C.D. D.K. and M.S. analyzed all experiments and together wrote the manuscript.

# DECLARATION OF INTERESTS

The authors declare no competing interests.

# STAR★METHODS

Detailed methods are provided in the online version of this paper and include the following:

- KEY RESOURCES TABLE
- EXPERIMENTAL MODEL
  - *C. elegans* maintenance
  - The CeMbio community
- METHOD DETAILS
  - Assessing bacterial susceptibility to neomycin
  - Harvesting and processing worms for colony forming units (CFUs) and next generation sequencing
  - Preparation of sequencing libraries
  - NGS data analysis
  - CFU counts
  - Bacterial genome sequence analyses
  - Generation of APH(3')-positive *Stenotrophomonas rhizophila* and *E. coli* strains
  - RNA extraction and RNA-seq analysis
  - Neomycin avoidance
  - Bacterial preference assays
  - Infection resistance assay
  - Lipid staining and quantification
  - Fluorescent image analysis
- QUANTIFICATION AND STATISTICAL ANALYSIS

# SUPPLEMENTAL INFORMATION

Supplemental information can be found online at <https://doi.org/10.1016/j.isci.2025.112209>.

Received: August 22, 2024  
Revised: January 9, 2025  
Accepted: March 10, 2025  
Published: March 13, 2025

# REFERENCES

1. Sommer, F., and Bäckhed, F. (2013). The gut microbiota-masters of host development and physiology. *Nat. Rev. Microbiol.* 11, 227–238. <https://doi.org/10.1038/nrmicro2974>.
2. Morais, L.H., Schreiber, H.L., and Mazmanian, S.K. (2021). The gut microbiota–brain axis in behaviour and brain disorders. *Nat. Rev. Microbiol.* 19, 241–255. <https://doi.org/10.1038/s41579-020-00460-0>.
3. Fan, Y., and Pedersen, O. (2021). Gut microbiota in human metabolic health and disease. *Nat. Rev. Microbiol.* 19, 55–71. <https://doi.org/10.1038/s41579-020-0433-9>.
4. Belkaid, Y., and Harrison, O.J. (2017). Homeostatic Immunity and the Microbiota. *Immunity* 46, 562–576. <https://doi.org/10.1016/j.immuni.2017.04.008>.
5. Shabat, S.K.B., Sasson, G., Doron-Faigenboim, A., Durman, T., Yaacoby, S., Berg Miller, M.E., White, B.A., Shterzer, N., and Mizrahi, I. (2016). Specific microbiome-dependent mechanisms underlie the energy harvest efficiency of ruminants. *ISME J.* 10, 2958–2972. <https://doi.org/10.1038/ismej.2016.62>.
6. Rosengaus, R.B., Zecher, C.N., Schultheis, K.F., Brucker, R.M., and Bordenstein, S.R. (2011). Disruption of the termite gut microbiota and its prolonged consequences for fitness. *Appl. Environ. Microbiol.* 77, 4303–4312. <https://doi.org/10.1128/AEM.01886-10>.
7. Shukla, S.P., Sanders, J.G., Byrne, M.J., and Pierce, N.E. (2016). Gut microbiota of dung beetles correspond to dietary specializations of adults and larvae. *Mol. Ecol.* 25, 6092–6106. <https://doi.org/10.1111/mec.13901>.
8. Gilbert, J.A., Blaser, M.J., Caporaso, J.G., Jansson, J.K., Lynch, S.V., and Knight, R. (2018). Current understanding of the human microbiome. *Nat. Med.* 24, 392–400. <https://doi.org/10.1038/nm.4517>.
9. Moran, N.A., McCutcheon, J.P., and Nakabachi, A. (2008). Genomics and evolution of heritable bacterial symbionts. *Annu. Rev. Genet.* 42, 165–190. <https://doi.org/10.1146/annurev.genet.41.110306.130119>.
10. Feyereisen, R. (2011). Arthropod CYPomes illustrate the tempo and mode in P450 evolution. *Biochim. Biophys. Acta* 1814, 19–28. <https://doi.org/10.1016/j.bbapap.2010.06.012>.
11. Ceja-Navarro, J.A., Vega, F.E., Karaoz, U., Hao, Z., Jenkins, S., Lim, H.C., Kosina, P., Infante, F., Northen, T.R., and Brodie, E.L. (2015). Gut microbiota mediate caffeine detoxification in the primary insect pest of coffee. *Nat. Commun.* 6, 7618. <https://doi.org/10.1038/ncomms8618>.
12. Kohl, K.D., Weiss, R.B., Cox, J., Dale, C., and Dearing, M.D. (2014). Gut microbes of mammalian herbivores facilitate intake of plant toxins. *Ecol. Lett.* 17, 1238–1246. <https://doi.org/10.1111/ele.12329>.
13. Shukla, S.P., and Beran, F. (2020). Gut microbiota degrades toxic isothiocyanates in a flea beetle pest. *Mol. Ecol.* 29, 4692–4705. <https://doi.org/10.1111/mec.15657>.
14. Alavanja, M.C.R., Hoppin, J.A., and Kamel, F. (2004). Health effects of chronic pesticide exposure: Cancer and neurotoxicity. *Annu. Rev. Public Health* 25, 155–197. <https://doi.org/10.1146/annurev.publhealth.25.101802.123020>.
15. Kikuchi, Y., Hayatsu, M., Hosokawa, T., Nagayama, A., Tago, K., and Fukatsu, T. (2012). Symbiont-mediated insecticide resistance. *Proc. Natl. Acad. Sci. USA* 109, 8618–8622. <https://doi.org/10.1073/pnas.1200231109>.
16. Itoh, H., Tago, K., Hayatsu, M., and Kikuchi, Y. (2018). Detoxifying symbiosis: Microbe-mediated detoxification of phytotoxins and pesticides in insects. *Nat. Prod. Rep.* 35, 434–454. <https://doi.org/10.1039/c7np00051k>.
17. Wang, G.H., Berdy, B.M., Velasquez, O., Jovanovic, N., Alkhalifa, S., Minbiole, K.P.C., and Brucker, R.M. (2020). Changes in Microbiome Confer Multigenerational Host Resistance after Sub-toxic Pesticide Exposure. *Cell Host Microbe* 27, 213–224.e7. <https://doi.org/10.1016/j.chom.2020.01.009>.
18. Wang, G.H., Dittmer, J., Douglas, B., Huang, L., and Brucker, R.M. (2021). Coadaptation between host genome and microbiome under long-term

- xenobiotic-induced selection. *Sci. Adv.* 7, eabd4473. <https://doi.org/10.1126/sciadv.abd4473>.
19. Douglas, A.E. (2019). Simple animal models for microbiome research. *Nat. Rev. Microbiol.* 17, 764–775. <https://doi.org/10.1038/s41579-019-0242-1>.
20. Shapira, M. (2017). Host–microbiota interactions in *Caenorhabditis elegans* and their significance. *Curr. Opin. Microbiol.* 38, 142–147. <https://doi.org/10.1016/j.mib.2017.05.012>.
21. Berg, M., Stenuit, B., Ho, J., Wang, A., Parke, C., Knight, M., Alvarez-Cohen, L., and Shapira, M. (2016). Assembly of the *Caenorhabditis elegans* gut microbiota from diverse soil microbial environments. *ISME J.* 10, 1998–2009. <https://doi.org/10.1038/ismej.2015.253>.
22. Berg, M., Zhou, X.Y., and Shapira, M. (2016). Host-specific functional significance of *Caenorhabditis* gut commensals. *Front. Microbiol.* 7, 1622. <https://doi.org/10.3389/fmicb.2016.01622>.
23. Samuel, B.S., Rowedder, H., Braendle, C., Félix, M.-A., and Ruvkun, G. (2016). *Caenorhabditis elegans* responses to bacteria from its natural habitats. *Proc. Natl. Acad. Sci.* 113, E3941–E3949. <https://doi.org/10.1073/pnas.1607183113>.
24. Berg, M., Monnin, D., Cho, J., Nelson, L., Crits-Christoph, A., and Shapira, M. (2019). TGF $\beta$ /BMP immune signaling affects abundance and function of *C. elegans* gut commensals. *Nat. Commun.* 10, 604. <https://doi.org/10.1038/s41467-019-08379-8>.
25. Ortiz, A., Vega, N.M., Ratzke, C., and Gore, J. (2021). Interspecies bacterial competition regulates community assembly in the *C. elegans* intestine. *ISME J.* 15, 2131–2145. <https://doi.org/10.1038/s41396-021-00910-4>.
26. Hoang, K.L., Choi, H., Gerardo, N.M., and Morran, L.T. (2022). Coevolution's conflicting role in the establishment of beneficial associations. *Evolution* 76, 1073–1081. <https://doi.org/10.1111/evo.14472>.
27. King, K.C., Brockhurst, M.A., Vasieva, O., Paterson, S., Betts, A., Ford, S.A., Frost, C.L., Horsburgh, M.J., Haldenby, S., and Hurst, G.D. (2016). Rapid evolution of microbe-mediated protection against pathogens in a worm host. *ISME J.* 10, 1915–1924. <https://doi.org/10.1038/ismej.2015.259>.
28. Petersen, C., Hamerich, I.K., Adair, K.L., Griem-Krey, H., Torres Oliva, M., Hoepfner, M.P., Bohannan, B.J.M., and Schulenburg, H. (2023). Host and microbiome jointly contribute to environmental adaptation. *ISME J.* 17, 1953–1965. <https://doi.org/10.1038/s41396-023-01507-9>.
29. Giordano-Santini, R., Milstein, S., Svrikapa, N., Tu, D., Johnsen, R., Bailie, D., Vidal, M., and Dupuy, D. (2010). An antibiotic selection marker for nematode transgenesis. *Nat. Methods* 7, 721–723. <https://doi.org/10.1038/nmeth.1494>.
30. Ley, R.E., Bäckhed, F., Turnbaugh, P., Lozupone, C.A., Knight, R.D., and Gordon, J.I. (2005). Obesity alters gut microbial ecology. *Proc. Natl. Acad. Sci. USA* 102, 11070–11075. <https://doi.org/10.1073/pnas.0504978102>.
31. Degrootola, A.K., Low, D., Mizoguchi, A., and Mizoguchi, E. (2016). Current understanding of dysbiosis in disease in human and animal models. *Inflamm. Bowel Dis.* 22, 1137–1150. <https://doi.org/10.1097/MIB.0000000000000750>.
32. Zhang, F., Berg, M., Dierking, K., Félix, M.A., Shapira, M., Samuel, B.S., and Schulenburg, H. (2017). *Caenorhabditis elegans* as a model for microbiome research. *Front. Microbiol.* 8, 485. <https://doi.org/10.3389/fmicb.2017.00485>.
33. Dirksen, P., Assié, A., Zimmermann, J., Zhang, F., Tietje, A.M., Marsh, S.A., Félix, M.A., Shapira, M., Kaleta, C., Schulenburg, H., and Samuel, B.S. (2020). CeMbio - The *Caenorhabditis elegans* microbiome resource. *G3 (Bethesda)*. 10, 3025–3039. <https://doi.org/10.1534/g3.120.401309>.
34. Dirksen, P., Marsh, S.A., Braker, I., Heitland, N., Wagner, S., Nakad, R., Mader, S., Petersen, C., Kowalik, V., Rosenstiel, P., et al. (2016). The native microbiome of the nematode *Caenorhabditis elegans*: gateway to a new host-microbiome model. *BMC Biol.* 14, 38. <https://doi.org/10.1186/s12915-016-0258-1>.
35. Wright, G.D., and Thompson, P.R. (1999). Aminoglycoside phosphotransferases: proteins, structure, and mechanism. *Front. Biosci.* 4, D9–D21. <https://doi.org/10.2741/wright>.
36. Zhang, Z., Liu, L., Twumasi-Boateng, K., Block, D.H.S., and Shapira, M. (2017). FOS-1 functions as a transcriptional activator downstream of the *C. elegans* JNK homolog KGB-1. *Cell. Signal.* 30, 1–8. <https://doi.org/10.1016/j.cellsig.2016.11.010>.
37. Mizuno, T., Hisamoto, N., Terada, T., Kondo, T., Adachi, M., Nishida, E., Kim, D.H., Ausubel, F.M., and Matsumoto, K. (2004). The *Caenorhabditis elegans* MAPK phosphatase VHP-1 mediates a novel JNK-like signaling pathway in stress response. *EMBO J.* 23, 2226–2234. <https://doi.org/10.1038/sj.emboj.7600226>.
38. Mizuno, T., Fujiki, K., Sasakawa, A., Hisamoto, N., and Matsumoto, K. (2008). Role of the *Caenorhabditis elegans* Shc Adaptor Protein in the c-Jun N-Terminal Kinase Signaling Pathway. *Mol. Cell Biol.* 28, 7041–7049. <https://doi.org/10.1128/mcb.00938-08>.
39. Melo, J.A., and Ruvkun, G. (2012). Inactivation of conserved *C. elegans* genes engages pathogen- and xenobiotic-associated defenses. *Cell* 149, 452–466. <https://doi.org/10.1016/j.cell.2012.02.050>.
40. Liu, L., Ruediger, C., and Shapira, M. (2018). Integration of stress signaling in *caenorhabditis elegans* through cell-nonautonomous contributions of the JNK homolog KGB-1. *Genetics* 210, 1317–1328. <https://doi.org/10.1534/genetics.118.301446>.
41. Pérez-Carrascal, O.M., Choi, R., Massot, M., Pees, B., Narayan, V., and Shapira, M. (2022). Host Preference of Beneficial Commensals in a Microbially-Diverse Environment. *Front. Cell. Infect. Microbiol.* 12, 1–9. <https://doi.org/10.3389/fcimb.2022.795343>.
42. Montalvo-Katz, S., Huang, H., Appel, M.D., Berg, M., and Shapira, M. (2013). Association with soil bacteria enhances p38-dependent infection resistance in *Caenorhabditis elegans*. *Infect. Immun.* 81, 514–520. <https://doi.org/10.1128/IAI.00653-12>.
43. Zhang, Y., Cheng, D., Xie, J., Zhang, Y., Wan, Y., Zhang, Y., and Shi, X. (2022). Impacts of farmland application of antibiotic-contaminated manures on the occurrence of antibiotic residues and antibiotic resistance genes in soil: A meta-analysis study. *Chemosphere* 300, 134529. <https://doi.org/10.1016/j.chemosphere.2022.134529>.
44. Cai, M., Wang, Z., Gu, H., Dong, H., Zhang, X., Cui, N., Zhou, L., Chen, G., and Zou, G. (2022). Occurrence and temporal variation of antibiotics and antibiotic resistance genes in hospital inpatient department wastewater: Impacts of daily schedule of inpatients and wastewater treatment process. *Chemosphere* 292, 133405. <https://doi.org/10.1016/j.chemosphere.2021.133405>.
45. Stockwell, V.O., and Duffy, B. (2012). Use of antibiotics in plant agriculture. *Rev. Sci. Tech.* 31, 199–210. <https://doi.org/10.20506/rst.31.1.2104>.
46. Farkas, A., Coman, C., Szekeres, E., Teban-Man, A., Carpa, R., and Butiuc-Keul, A. (2022). Molecular Typing Reveals Environmental Dispersion of Antibiotic-Resistant Enterococci under Anthropogenic Pressure. *Antibiotics* 11, 1213. <https://doi.org/10.3390/antibiotics11091213>.
47. Ullmann, I.F., Tunsjo, H.S., Andreassen, M., Nielsen, K.M., Lund, V., and Charnock, C. (2019). Detection of aminoglycoside resistant bacteria in sludge samples from Norwegian drinking water treatment plants. *Front. Microbiol.* 10, 1–12. <https://doi.org/10.3389/fmicb.2019.00487>.
48. Lester, C.H., Frimodt-Moller, N., and Hammerum, A.M. (2004). Conjugal transfer of aminoglycoside and macrolide resistance between *Enterococcus faecium* isolates in the intestine of streptomycin-treated mice. *FEMS Microbiol. Lett.* 235, 385–391. <https://doi.org/10.1016/j.femsle.2004.04.050>.
49. Vitali, L.A., Petrelli, D., Lamikanra, A., Prenna, M., and Akinkunmi, E.O. (2014). Diversity of antibiotic resistance genes and staphylococcal cassette chromosome mec elements in faecal isolates of coagulase-negative staphylococci from Nigeria. *BMC Microbiol.* 14, 106. <https://doi.org/10.1186/1471-2180-14-106>.

50. Twumasi-Boateng, K., Wang, T.W., Tsai, L., Lee, K.H., Salehpour, A., Bhat, S., Tan, M.W., and Shapira, M. (2012). An age-dependent reversal in the protective capacities of JNK signaling shortens *Caenorhabditis elegans* lifespan. *Aging Cell* 11, 659–667. <https://doi.org/10.1111/j.1474-9726.2012.00829.x>.
51. Vind, A.C., Genzor, A.V., and Bekker-Jensen, S. (2020). Ribosomal stress-surveillance: Three pathways is a magic number. *Nucleic Acids Res.* 48, 10648–10661. <https://doi.org/10.1093/nar/gkaa757>.
52. Hollos, P., Marchisella, F., and Coffey, E.T. (2018). JNK Regulation of Depression and Anxiety. *Brain Plast.* 3, 145–155. <https://doi.org/10.3233/bpl-170062>.
53. Jones, K.T., Greer, E.R., Pearce, D., and Ashrafi, K. (2009). Rictor/torc2 regulates *Caenorhabditis elegans* fat storage, body size, and development through *sgk-1*. *PLoS Biol.* 7, e60–e0615. <https://doi.org/10.1371/journal.pbio.1000060>.
54. Lee, J.Y., Tsois, R.M., and Bäuml, A.J. (2022). The microbiome and gut homeostasis. *Science* 377, eabp9960. <https://doi.org/10.1126/science.abp9960>.
55. Vijay-kumar, M., Aitken, J.D., Carvalho, F.A., Cullender, T.C., Mwangi, S., Srinivasan, S., Sitaraman, S.V., Knight, R., Ley, R.E., and Gewirtz, A.T. (2010). Metabolic syndrome and altered gut microbiota in mice lacking Toll-like receptor 5. *Science* 328, 228–231. <https://doi.org/10.1126/science.1179721>.
56. Ihara, S., Hirata, Y., Serizawa, T., Suzuki, N., Sakitani, K., Kinoshita, H., Hayakawa, Y., Nakagawa, H., Ijichi, H., Tateishi, K., and Koike, K. (2016). TGF- $\beta$  Signaling in Dendritic Cells Governs Colonic Homeostasis by Controlling Epithelial Differentiation and the Luminal Microbiota. *J. Immunol.* 196, 4603–4613. <https://doi.org/10.4049/jimmunol.1502548>.
57. Dabke, K., Hendrick, G., and Devkota, S. (2019). The gut microbiome and metabolic syndrome. *J. Clin. Investig.* 129, 4050–4057. <https://doi.org/10.1172/JCI129194>.
58. Turnbaugh, P.J., Ley, R.E., Mahowald, M.A., Magrini, V., Mardis, E.R., and Gordon, J.I. (2006). An obesity-associated gut microbiome with increased capacity for energy harvest. *Nature* 444, 1027–1031. <https://doi.org/10.1038/nature05414>.
59. Soen, Y., Knafo, M., and Elgart, M. (2015). A principle of organization which facilitates broad Lamarckian-like adaptations by improvisation. *Biol. Direct* 10, 68. <https://doi.org/10.1186/s13062-015-0097-y>.
60. Shapira, M., Hamlin, B.J., Rong, J., Chen, K., Ronen, M., and Tan, M.W. (2006). A conserved role for a GATA transcription factor in regulating epithelial innate immune responses. *Proc. Natl. Acad. Sci. USA* 103, 14086–14091. <https://doi.org/10.1073/pnas.0603424103>.
61. Innes, R.W., Bent, A.F., Kunkel, B.N., Bisgrove, S.R., and Staskawicz, B.J. (1993). Molecular analysis of avirulence gene *avrRpt2* and identification of a putative regulatory sequence common to all known *Pseudomonas syringae* avirulence genes. *J. Bacteriol.* 175, 4859–4869. <https://doi.org/10.1128/jb.175.15.4859-4869.1993>.
62. Bolyen, E., Rideout, J.R., Dillon, M.R., Bokulich, N.A., Abnet, C.C., Al-Ghalith, G.A., Alexander, H., Alm, E.J., Arumugam, M., Asnicar, F., et al. (2019). Reproducible, interactive, scalable and extensible microbiome data science using QIIME 2. *Nat. Biotechnol.* 37, 852–857. <https://doi.org/10.1038/s41587-019-0209-9>.
63. Love, M.I., Huber, W., and Anders, S. (2014). Moderated estimation of fold change and dispersion for RNA-seq data with DESeq2. *Genome Biol.* 15, 550–621. <https://doi.org/10.1186/s13059-014-0550-8>.
64. Schneider, C.A., Rasband, W.S., and Eliceiri, K.W. (2012). NIH Image to ImageJ: 25 years of image analysis. *Nat. Methods* 9, 671–675. <https://doi.org/10.1038/nmeth.2089>.
65. Bray, N.L., Pimentel, H., Melsted, P., and Pachter, L. (2016). Near-optimal probabilistic RNA-seq quantification. *Nat. Biotechnol.* 34, 525–527. <https://doi.org/10.1038/nbt.3519>.
66. Sun, J., Lu, F., Luo, Y., Bie, L., Xu, L., and Wang, Y. (2023). OrthoVenn3: An integrated platform for exploring and visualizing orthologous data across genomes. *Nucleic Acids Res.* 51, W397–W403. <https://doi.org/10.1093/nar/gkad313>.
67. Wickham, H. (2016). *Ggplot2: Elegant Graphics for Data Analysis* (Springer-Verlag), pp. 79–84. <https://doi.org/10.1007/978-3-319-24277-4>.
68. Therneau, T. (2024). *A Package for Survival Analysis in R* (R Package), pp. 148–149. <https://doi.org/10.32614/CRAN.package.survival>.
69. Mcmurdie, P.J., and Holmes, S. (2013). phyloseq: An R Package for Reproducible Interactive Analysis and Graphics of Microbiome Census Data. *PLoS One* 8, e61217. <https://doi.org/10.1371/journal.pone.0061217>.
70. Pohlert, T. (2014). The Pairwise Multiple Comparison of Mean Ranks Package (PMCMR). *R Package*, 2–5. <https://doi.org/10.32614/CRAN.package.PMCMR>.
71. McArthur, A.G., Waglechner, N., Nizam, F., Yan, A., Azad, M.A., Baylay, A.J., Bhullar, K., Canova, M.J., De Pascale, G., Ejim, L., et al. (2013). The comprehensive antibiotic resistance database. *Antimicrob. Agents Chemother.* 57, 3348–3357. <https://doi.org/10.1128/AAC.00419-13>.
72. Edgar, R.C. (2010). Search and clustering orders of magnitude faster than BLAST. *Bioinformatics* 26, 2460–2461. <https://doi.org/10.1093/bioinformatics/btq461>.
73. Shapira, M., and Tan, M.-W. (2008). Genetic analysis of *Caenorhabditis elegans* innate immunity. *Methods Mol. Biol.* 415, 429–442. [https://doi.org/10.1007/978-1-59745-570-1\\_25](https://doi.org/10.1007/978-1-59745-570-1_25).
74. Escorcía, W., Ruter, D.L., Nhan, J., and Curran, S.P. (2018). Quantification of lipid abundance and evaluation of lipid distribution in *Caenorhabditis elegans* by Nile red and oil red O staining. *J. Vis. Exp.* 1–6, 57352. <https://doi.org/10.3791/57352>.
75. Matty, M.A., Lau, H.E., Haley, J.A., Singh, A., Chakraborty, A., Kono, K., Reddy, K.C., Hansen, M., and Chalasani, S.H. (2022). Intestine-to-neuronal signaling alters risk-taking behaviors in food-deprived *Caenorhabditis elegans*. *PLoS Genet.* 18, e1010178. <https://doi.org/10.1371/journal.pgen.1010178>.
76. Schindelin, J., Arganda-Carreras, I., Frise, E., Kaynig, V., Longair, M., Pietzsch, T., Preibisch, S., Rueden, C., Saalfeld, S., Schmid, B., et al. (2012). Fiji: An open-source platform for biological-image analysis. *Nat. Methods* 9, 676–682. <https://doi.org/10.1038/nmeth.2019>.



## STAR★METHODS

### KEY RESOURCES TABLE

REAGENT or RESOURCE	SOURCE	IDENTIFIER
<b>Bacterial and virus strains</b>		
<i>E. coli</i> OP50	CGC	OP50, WBStrain00041969
<i>E. coli</i> OP50 transformed with APH(3')-encoding plasmid pVSP61	This study, see below	N/A
<i>Enterobacter hormaechei</i> CEent1	CGC, Dirksen et al. <sup>33</sup>	CEent1, WBStrain00047224
<i>Lelliottia amnigena</i> JUb66	CGC, Dirksen et al. <sup>33</sup>	JUb66, WBStrain00047336
<i>Acinetobacter guillouiae</i> MYb10	CGC, Dirksen et al. <sup>33</sup>	MYb10, WBStrain00047356
<i>Sphingomonas molluscorum</i> JUb134	CGC, Dirksen et al. <sup>33</sup>	JUb134, WBStrain00047337
<i>Stenotrophomonas indicatrix</i> JUb19	CGC, Dirksen et al. <sup>33</sup>	JUb19, WBStrain00047334
<i>Pseudomonas lurida</i> MYb11	CGC, Dirksen et al. <sup>33</sup>	MYb11, WBStrain00047357
<i>Pseudomonas berkeleyensis</i> MSPm1	CGC, Dirksen et al. <sup>33</sup>	MSPm1, WBStrain00047354
<i>Comamonas piscis</i> BIGb0172	CGC, Dirksen et al. <sup>33</sup>	BIGb0172, WBStrain00047214
<i>Pantoea nemavictus</i> BIGb0393	CGC, Dirksen et al. <sup>33</sup>	BIGb0393, WBStrain00047215
<i>Ochrobactrum vermis</i> MYb71	CGC, Dirksen et al. <sup>33</sup>	MYb71, WBStrain00047358
<i>Sphingobacterium multivorum</i> BIGb0170	CGC, Dirksen et al. <sup>33</sup>	BIGb0170, WBStrain00047213
<i>Chryseobacterium scophthalmum</i> JUb44	CGC, Dirksen et al. <sup>33</sup>	JUb44, WBStrain00047335
<i>Stenotrophomonas rhizophila</i> BIGb262	Buck Samuel's lab, Baylor College of Medicine, Houston TX	BIGb262
<i>Stenotrophomonas rhizophila</i> BIGb262 transformed with APH(3')-encoding plasmid pVSP61	This study	BIGb262 APH(3')+
<i>Pseudomonas aeruginosa</i> PA14-GFP	Jonathan Ewbank's lab, Shapira et al. <sup>60</sup>	PA14-GFP
<b>Chemicals, peptides, and recombinant proteins</b>		
AMPure XP Reagent, 60 mL	Beckman Coulter	Cat#A63881
Bleach (Sodium Hypochlorite)	Sigma-Aldrich	Cat#425044
dNTP set 10mM	Invitrogen	Cat#18427013
Cholesterol	Sigma	Cat#C8667
KH <sub>2</sub> PO <sub>4</sub>	Fisher Scientific	Cat#P285-500
Kanamycin Sulfate	Gibco	Cat#11815-024
Levamisole Hydrochloride	Fisher Scientific	Cat#AC187870100
MgSO <sub>4</sub>	Fisher Scientific	Cat#M63-500
Na <sub>2</sub> HPO <sub>4</sub>	Fisher Scientific	Cat#S374-500
NaCl	Fisher Scientific	Cat#S271-3
Neomycin Trisulfate	Sigma	Cat#N1876
Isopropanol	Fisher Chemical	Cat#A451-4
Bacto-Tryptone	Becton, Dickinson	Cat#211705
Yeast Extract	Gibco	Cat#DF0127-17-9
Difco Agar	Becton, Dickinson	214010
Bacto-peptone	Becton, Dickinson	Cat#DF0118-17-0
Na <sub>2</sub> HPO <sub>4</sub>	Fisher Chemical	Cat#S374-500
CaCl <sub>2</sub>	Fisher Chemical	Cat#C79-500
Trizol	Ambion	Cat#15596026
Agarose, low melting	Sigma	Cat#A9539

(Continued on next page)



# Continued

REAGENT or RESOURCE	SOURCE	IDENTIFIER
Chloroform	Fisher Chemical	Cat#C298-1
Triton X-100	Fisher Scientific	Cat#BP-151
NaOH (10N)	Teknova	Cat#N4710
PBS	Gibco	Cat#10010023
Oil Red O solution	Sigma	Cat#O9755

# Deposited data

Full genome: BIGb262 <i>Stenotrophomonas rhizophila</i>	Michael Herman's lab, University of Nebraska, Lincoln	NCBI: PRJNA986126
RNA-seq raw data: N2 worms on OP50 with or without neomycin	This study	GEO: GSE246966

# Experimental models: Organisms/strains

<i>C. elegans</i> strain Bristol N2	CGC	N2
<i>C. elegans</i> strain KU21: <i>kgb-1(km21)</i>	CGC	KU21
<i>C. elegans</i> strain KU25: <i>pmk-1(km25)</i>	CGC	KU25
<i>C. elegans</i> strain KU4: <i>sek-1(km4)</i>	CGC	KU4
<i>C. elegans</i> strain ZD2520: <i>mek-1(qd374)</i>	Dennis Kim's lab	ZD2520

# Oligonucleotides

Primer for V4 amplification: TCGTCGGCAGC GTCAGATGTGTATAAGAGACAGGTGCCAG CMGCCGCGGTAA	Illumina, synthesized at IDT	Tailed 515(F)
Primers for V4 amplification: GTCTCGTGGGCTCGGAGATGTGTATAAGA GACAGGGACTACHVGGGTWTCTAAT	Illumina, synthesized at IDT	Tailed 806(F)

# Recombinant DNA

Plasmid: pVSP61, encoding mRFP-1 and APH(3')	Goodrich-Blair's lab, University of Tennessee, Innes et al. <sup>61</sup>	pVSP61
--	--	--------

# Software and algorithms

Qiime2	Bolyen et al. <sup>62</sup>	<a href="https://qiime2.org">https://qiime2.org</a>
DESeq2	Love et al. <sup>63</sup>	<a href="https://github.com/thelovelab/DESeq2">https://github.com/thelovelab/DESeq2</a>
ImageJ	Schneider et al. <sup>64</sup>	<a href="https://imagej.net/ij/">https://imagej.net/ij/</a>
Kallisto	Bray et al. <sup>65</sup>	<a href="https://pachterlab.github.io/kallisto/download">https://pachterlab.github.io/kallisto/ download</a> <a href="https://pachterlab.github.io/kallisto/about">https://pachterlab.github.io/ kallisto/about</a>
OrthoVenn3	Sun et al. <sup>66</sup>	<a href="https://orthovenn3.bioinfotoolkits.net/">https://orthovenn3.bioinfotoolkits.net/</a>
ggplot2	Hadley Wickham <sup>67</sup>	<a href="https://ggplot2.tidyverse.org/">https://ggplot2.tidyverse.org/</a>
Survival analyses	Terry Therneau <sup>68</sup>	<a href="https://cran.r-project.org/web/packages/survival/index.html">https://cran.r-project.org/web/packages/ survival/index.html</a>
Phyloseq	McMurdie et al. <sup>69</sup>	<a href="https://joey711.github.io/phyloseq/">https://joey711.github.io/phyloseq/</a>
PMCMRplus (ANOVA analyses)	Thorsten Pohlert <sup>70</sup>	<a href="https://cran.r-project.org/web/packages/PMCMRplus/index.html">https://cran.r-project.org/web/packages/ PMCMRplus/index.html</a>
Comprehensive Antibiotic Resistance Database (CARD)	McArthur et al. <sup>71</sup>	<a href="https://card.mcmaster.ca">https://card.mcmaster.ca</a>

# Other

DNeasy PowerSoil Pro Kit	Qiagen	Cat#47016
Miniseq High Output Reagent Kit	Illumina	Cat#FC-420-1003
Nextera XT DNA Library Preparation Kit	Illumina	Cat#FC-131-1096
Nextera XT Index Kit v2 Set A	Illumina	Cat#FC-131-2001
PhiX Control v3	Illumina	Cat#FC-110-3001
Phusion High-Fidelity DNA Polymerase	New England Biolabs	Cat#M0530L
Qubit dsDNA HS Assay kit	Invitrogen	Cat#Q32851

(Continued on next page)

**Continued**

REAGENT or RESOURCE	SOURCE	IDENTIFIER
Zirconia/Silica Beads 1.0 mm diameter	Fisher Scientific	Cat#NC9847287
KAPA HiFi HotStart ReadyMix	Roche	Cat#07958935001

## EXPERIMENTAL MODEL

### *C. elegans* maintenance

*C. elegans* worms were maintained at 20°C on Nematode Growth Medium (NGM) plates seeded with *E. coli* bacteria strain OP50. NGM: 3 g/L NaCl, 2.5 g/L Bacto-peptone and 17 g/L Bacto-agar are dissolved in Milli-Q filtered water, autoclaved. After cooling to 55°C, 1 mL/L cholesterol (stock solution: 5 mg/mL in ethanol), 25 mL/L of 1M potassium phosphate, 1 mL/L of 1M magnesium sulfate and 1 mL calcium chloride (1M) are added. Where designated, antibiotic was also added after autoclaving. Germ-free and synchronized populations of arrested L1 larvae were obtained by bleaching gravid worms with a 1.8% sodium hypochlorite 0.375 M KOH solution for 6 min (with vigorous shaking), to dissolve mothers and release their eggs, and hatching eggs on NGM without bacteria food. Worms were subsequently raised to adulthood at 20°C on plates with bacterial monocultures or communities in large excess.

### The CeMbio community

CeMbio is a defined community of twelve characterized and genome-sequenced worm gut commensals<sup>33</sup> Genome sequences of CeMbio strains are available in the European Nucleotide Archive (accession number PRJEB37895). In setting for an experiment, individual strains were grown at 28°C for two days, shaking, in 2 mL of LB. Saturated cultures of each monoculture were adjusted to OD<sub>600nm</sub> of 4, mixed in desired combinations (or kept as individual strains) and spread as lawns on nematode growth media (NGM) plates with or without antibiotics.

A bacterial community reconfigured to mimic the gut community as assembled from CeMbio in worms exposed to neomycin, included JUb19, MYb71, and BIGb0172 in a ratio of 9: 0.27: 0.5, respectively.

## METHOD DETAILS

### Assessing bacterial susceptibility to neomycin

#### Growth inhibition on plates

Sterile paper disks soaked in solutions with different antibiotic concentrations were placed on bacterial lawns seeded from 0.05 OD<sub>600nm</sub> cultures on LB plates and incubated overnight at 28°C. Bacterial sensitivity to antibiotic was assessed by the width of the clear halo around the disk.

#### Growth in liquid

Individual strains, diluted from saturated cultures to 0.05 OD<sub>600nm</sub>, were raised in LB at 28°C in wells of a microtiter plate containing different antibiotic concentrations, and their growth monitored during 48 h with OD<sub>600nm</sub> readings every 5 min using a Molecular Devices Versamax plate reader. Maximal growth rate was calculated to assess antibiotic sensitivity.

### Neomycin concentrations

Most experiments were carried out with 0.25 mg/mL neomycin, which was found to have clear physiological effects on worms (survival, avoidance). In experiments used for 16S rRNA analysis, a lower concentration of 0.1 mg/mL was selected, which has lower impact on host physiology (see Figure 1B) and may allow more nuanced analysis of changes in microbiome composition.

### *C. elegans* survival on neomycin

Worms were raised on OP50, CeMbio, or individual CeMbio strains until the first day of gravid, washed off plates and washed three times with 15 mL filter-sterilized M9 (3 g KH<sub>2</sub>PO<sub>4</sub>, 6 g Na<sub>2</sub>HPO<sub>4</sub>, 5 g NaCl, 1 mL 1 M MgSO<sub>4</sub>, H<sub>2</sub>O to 1 L. Sterilized by autoclaving.) before transferring to NGM plates with neomycin, and with *E. coli* as food, on which survival was scored. In experiments testing the ability of dead bacteria to protect worms from neomycin, killing was achieved by a 45 min incubation at 37°C with 1% paraformaldehyde, followed by washing five times with 15 mL filter-sterilized M9. Killing was verified by streaking a swab taken from lawn of dead bacteria on an LB plate, noting no growth.

### Harvesting and processing worms for colony forming units (CFUs) and next generation sequencing

Worms raised on CeMbio were washed five times with 1 mL M9-T (M9 + 0.025% Triton X-100), to remove surface adherent bacteria. They were then left in 100 µL M9-T for 10 min, to allow clearance of transient colonizers, before adding 100 µL of 10 mM levamisole solution to paralyze them. Thereafter, worms were surface-sterilized by the addition of 200 µL 4% bleach solution for 2 min and subsequently washed with 1 mL PBS twice to remove excess bleach and levamisole. Surface-sterilized worms (10–15 worms in 250 µL of M9) were ground by vortexing at full speed for 10 min with zirconia beads to release live bacteria, while monitoring worm degradation under a light microscope. After serial dilutions, aliquots were plated on LB plates +/- neomycin and incubated at 28°C for 2–3 days.

For next generation sequencing, washed worms were used for DNA extraction using the DNeasy PowerSoil Kit. DNA was similarly extracted from swabs taken of the bacterial lawns.

### Preparation of sequencing libraries

Extracted DNA was used as template (>1 ng per reaction) for amplification of the 16S rRNA V4 region, using tailed 515F and 806R primers, compatible with the Nextera XT DNA library prep kit (Illumina, FC-131-2001), and KAPA HiFi HotStart polymerase (Roche, #07958935001). Amplification was carried out as follows: 95°C for 3 min, 25 cycles of 95°C for 30 s, 55°C for 30 s and 72°C for 30 s, and 72°C for 5 min. PCR products were purified using the AMPure XP reagent. Indices were added using the Nextera kit, according to the manufacturer instructions and products cleaned again using AMPure XP reagent. Libraries prepared from different samples were combined in equimolar ratios as suggested by the Illumina manual and used in paired-end next generation sequencing (NGS) using an Illumina MiniSeq.

### NGS data analysis

Analysis of 16S rRNA amplicon data were conducted using QIIME2.<sup>62</sup> In total, 96.9% of the total reads passed quality filtering with an average read of 81200 reads per sample. Sequences were aligned and clustered into operational taxonomic units (OTU) based on the closed reference OTU picking algorithm using the QIIME2 implementation of UCLUST<sup>72</sup> and the taxonomy of each OTU was assigned based on 99% similarity to reference sequences based on 16S rRNA sequences, available in the *Caenorhabditis* Genetics Center, of CeMbio strains.

### CFU counts

CFUs of *Ochrobactrum* and *Stenotrophomonas* were counted on LB plates with 0.1 mg/mL neomycin based on their distinct morphologies: small and dark colonies for *Ochrobactrum*, large and orangish for *Stenotrophomonas* (Figure S3A). Estimates for total bacterial load relied on CFU counts on LB plates without antibiotics. In assessing gut persistence of CeMbio members during infection, CFUs of the latter were distinguished from those of the pathogen *P. aeruginosa* PA14-GFP based on their lack of fluorescence.

### Bacterial genome sequence analyses

Scanning of bacterial genomes for potential antibiotic resistance genes was performed using the Comprehensive Antibiotic Resistance Database (CARD).<sup>71</sup> The genome sequence of BIGb262 was provided by Michael Herman, from the University of Nebraska (NCBI accession number PRJNA986126). Comparison of the JUb19 and BIGb262 genomes was carried out using OrthoVenn3, identifying orthologous gene clusters to assess the evolutionary relatedness of the two species.<sup>66</sup> In addition, gene annotations for all four Neo-resistant strains were searched for aminoglycoside resistance genes in their corresponding NCBI entries.

### Generation of APH(3')-positive *Stenotrophomonas rhizophila* and *E. coli* strains

*Stenotrophomonas rhizophila* cells were made electrocompetent by incubating early exponential cultures on ice for 30 min, centrifuging at 4000g (4°C, 5 min), washing cell pellets with ice-cold 10% glycerol (v/v), resuspending in the same glycerol solution to a final concentration of  $2 \times 10^8$  cells/ml, and storing as aliquots at -80°C. For electroporation, 50  $\mu$ L aliquots of electrocompetent cells were each mixed with 2  $\mu$ L plasmid DNA (100 ng/ $\mu$ L, pVSP61 - a broad host range plasmid encoding mRFP-1 and APH(3')<sup>61</sup>). Cell/DNA mixtures were transferred to a chilled 0.1-cm cuvette and electroporated using a Bio-rad Gene Pulser, set at Ec1 ( $V = 1.8$  kV). Following recovery of 1 h in 1 mL LB at 28°C, 100  $\mu$ L were spread on LB plates with 0.1 mg/mL neomycin and incubated at 28°C.

OP50 was transformed with the same plasmid using the heat shock protocol. Competent cells were prepared from OD<sub>600</sub> 0.25–0.3 cultures by chilling on ice for 15 min, centrifuging at 4000 g at 4°C for 5 min, resuspending pellets in ice-cold 0.1 M CaCl<sub>2</sub> solution and incubating on ice for additional 30 min, then centrifuging again and resuspending pellets in 5 mL ice-cold 0.1 M CaCl<sub>2</sub> with 15% glycerol. Aliquots were stored at 80°C. For heat shock transformation, thawed 50- $\mu$ L aliquots of competent cells were mixed with 10 ng of plasmid DNA and incubated on ice for 30 min. Mixtures were then heat-shocked at 42°C for 45 s, moved to ice for 2 min, and then allowed to recover by addition of 450  $\mu$ L LB and incubation at 37°C with shaking for 1 h. Aliquots of 100  $\mu$ L from each tube were spread on LB plate with 0.1 mg/mL neomycin and incubated overnight at 37°C giving rise to neomycin resistant bacteria, also observed under aa fluorescence scope as red.

### RNA extraction and RNA-seq analysis

Synchronized worm populations were raised from L1 to adulthood at 20°C on NGM plates seeded with *E. coli*. Gravid worms were transferred to similar plates with or without 0.25 mg/mL neomycin for 8 h, following which 100–150 worms (per group, per replicate) were washed off, washed three times with M9 solution, snap-frozen with 1 mL Trizol, and stored at -80°C for further use. RNA extraction started with three rounds of freeze/thaw using liquid nitrogen and a dry bath set at 37°C. Following the final thaw, 200  $\mu$ L chloroform were added to each sample, vortexed, and the aqueous phase was collected. Molecular grade isopropanol was added at an equivalent volume of the collected aqueous phase and samples were centrifuged in a minicentrifuge at 14,000 rpm for 5 min at 4°C. Pellets were washed once with 500  $\mu$ L nuclease-free 75% EtOH, air-dried for 5–10 min, and subsequently resuspended in 45  $\mu$ L nuclease-free water. Genomic DNA contamination was removed using Turbo DNase (Qiagen). Extracted RNA samples were stored at -80°C. Total RNA was sent for sequencing to Novogene (<https://www.novogene.com/amea-en/>), where mRNA was purified from

total RNA using polyT oligos attached to magnetic beads, followed by cDNA synthesis using random hexamer primers, and 150 bp paired-end sequencing with an Illumina Novaseq 6000. Following removal of adaptor sequences and low quality reads, 23,990,910 reads/sample remained on average. Kallisto was employed to identify and quantify transcripts, and DESeq2 was used to identify differentially expressed genes, with a false-discovery-rate-corrected  $p$ -value cutoff of 0.05.<sup>63,65</sup> Gene Ontology analysis was performed using Generic GO term Finder (<https://go.princeton.edu>), with Bonferroni correction for  $p$ -values. RNA-seq raw data are available at GEO (GSE246966).

### Neomycin avoidance

Worms were grown on 60 mm diameter plates, with a lawn of food *E. coli*, covering about 60–70% of its center area. When worms reached adulthood, 30  $\mu$ L of neomycin solution in designated concentrations were spotted in the center of the plate. Images were captured 1 h later, using a Leica MZ16F stereoscope equipped with a Qimaging Micropublisher 5.0 camera, and the distance of worms from the point of antibiotic application was measured using ImageJ.

### Bacterial preference assays

Bacterial strains/communities were normalized to 4 OD<sub>600</sub> and further concentrated 2-fold in M9. 30  $\mu$ L of the concentrated culture were seeded on opposite sides of a 60 mm NGM plate in pairwise choice assays, or around plates periphery in multiple choice assays, providing excess food for developing worms. L1 worms were transferred to the center of plates, raised to adulthood at 20°C (40 h after transfer), at which point their number (#) in the vicinity of bacterial strains/communities was counted and used for calculating preference index: (# of worms near strain A – # near strain B)/total # of worms.

### Infection resistance assay

Worms raised on monocultures or bacterial communities until gravid were washed off and washed with 15mL filter-sterilized M9 solution three times, transferred to slow killing plates (SKP) with PA14-GFP. Survival assays were performed by counting dead and live worms each day, while removing the dead worms and censoring worms found dehydrated on plate walls.<sup>73</sup> Persistence of CeMbio members during infection was measured by CFU counts of colonies without GFP fluorescence. Differences were assessed using Kaplan-Meier estimator and post-hoc log -rank tests using the R *Survival* package.

### Lipid staining and quantification

Gravid worms raised on different bacterial strains/communities were washed off plates, washed three times in PBST (PBS +0.01% Triton X-100), fixed in 40% isopropanol by 3 min incubation at room temperature and incubated with 3 mg/mL Oil Red O solution in 60% isopropanol for 2 h at room temperature, followed by two washes, 30 min each, with PBST.<sup>74</sup> Images of stained worms were captured using a Leica MZ16F stereoscope equipped with a Qimaging Micropublisher 5.0 camera. Images were quantified using color deconvolution in ImageJ, normalizing to background and to an unstained head region. Within each experiment the same thresholds were used for normalization in all images and across the different groups.<sup>75</sup>

### Fluorescent image analysis

Fluorescent signal in images presented in Figure S9 was quantified by Fiji plugin within the ImageJ package.<sup>76</sup> Fluorescent signal per worm was calculated using Integrated Density values, from which background mean gray values and autofluorescence were subtracted, and subsequently normalized for worm size.<sup>41</sup>

## QUANTIFICATION AND STATISTICAL ANALYSIS

Survival curves were compared using Kaplan Meier Analysis and a post-hoc Log -rank test with asterisks defined in figure legends. All other comparisons were evaluated using Student's  $t$  test or with ANOVA followed by Tuckey's post hoc tests, as described in figure legends. Assumption of equal variance or unequal variance made no difference for calculated statistical significance.